Articles

Alkali Metal Cation Selectivity of [1$_7$]Ketonand in Methanol: Free Energy Perturbation and Molecular Dynamics Simulation Studies

Sungu Hwang, Yun Hee Jang,† Gean Ha Ryu,‡ and Doo Soo Chung*

Department of Chemistry, Seoul National University, Seoul 151-742, Korea
Received July 7, 1999

Free energy perturbation and molecular dynamics simulations were carried out to investigate the relative binding affinities of [1-]ketonand (**1**) toward alkali metal cations in methanol. The binding affinities of **1** toward the alkali metal cations were calculated to be in the order $Li^+ > Na^+ > K^+ > Rb^+ > Cs^+$, whereas our recent theoretically predicted and experimentally observed binding affinities for [1$_8$]starand (**2**) were in the order $K^+ > Rb^+ > Cs^+ > Na^+ > Li^+$. The extremely different affinities of **1** and **2** toward smaller cations, Li^+ and Na^+, were explained in terms of the differences in their ability to change the conformation to accommodate cations of different sizes. The carbonyl groups constituting the central cavity of **1** can reorganize to form a cavity with the optimal M^+–O distance, even for the smallest Li^+, without imposing serious strain on **1**. The highest affinity of **1** for Li^+ was predominantly due to the highest Coulombic attraction between the smallest Li^+ and the carbonyl oxygens of **1**.

Introduction

Macrocyclic molecules have received much attention because they can form a binding cavity for specific ligands and possess host–guest complexation properties, providing insight into the molecular recognition process especially in biological systems. In particular, the design of macrocycles featuring metal cation complexation with high stability and selectivity is a topic of growing interest not only due to its relevance to many biochemical processes but also because of many possible applications in various areas.[1-4] They can serve as model compounds for ion carriers in membranes,[5] metalloenzymes,[1] ion-binding proteins,[1] and ion channels,[6] and play a central role in establishing a rigorous understanding of the chemistry underlying the biological processes of these receptors.[1,3] Some examples in various fields of chemistry, physics, medicine, and environmental remediation[4,7] include: (1) use in the immobilization of radioactive Rb^+ for organ imaging and in the delivery of therapeutic doses of radionuclide (e.g. $^{111}Ag^+$ or $^{224}Ra^{2+}$) to tumor sites, where the subsequent decay of the radionuclide inactivates tumor cells; (2) use of chromoionophores consisting of a chromophore linked to an ionophore as selective optical sensors toward specific cations, in which a measurable change in the photochemical properties of the chromophore upon ion binding of the ionophore serves as a signal to specific ion recognition;[8] (3) use in the separation of radionuclides such as $^{137}Cs^+$ and $^{90}Sr^{2+}$, two major generators of heat in nuclear waste which complicates the disposal from waste streams. These synthetic ionophores usually achieve selectivity through their rigid and preorganized cavities. Recently, Lee and coworkers[9-12] have synthesized a series of [1$_n$]ketonands and [1$_n$]starands of which [1$_7$]ketonand (**1**) and [1$_8$]starand (**2**) are shown in Figure 1. Also we have reported the synthesis of [1$_4$]ketonand,[13] and the theoretical study on the isomerism between [1$_n$]ketonand and [1$_n$]starand.[14] An *ab initio* study on the relative stability between [1$_n$]ketonand and [1$_n$]starand for $n = 4$, and 6 was also reported.[15] These novel and highly preorganized macrocycles were expected to form stable complexes selectively with specific alkali metal cations.[9-12] Cui *et al.* reported an *ab initio* study on the alkali metal cation affinities and selectivity of a model compound representing [1$_6$]starand in the gas phase.[16] We recently reported a combined study of an FEP simulation and an NMR titration experiment on the relative binding affinity of **2** in methanol solvent.[17] The selectivity determined in the NMR experiment was in the order $K^+ > Rb^+ > Cs^+ > Na^+ > Li^+$, and this was in excellent agreement with the FEP simulation results.[17]

Here we report a theoretical calculation on the complexation behavior of **1** with alkali metal cations to elucidate their relative binding affinities toward the alkali cations. The theoretical study of host–guest systems can offer information on the active conformation of the host in complexing with the guest and on the molecular-level interpretation of the experimental data.[18] This in turn permits a much higher predictiveness in designing a novel macrocyclic host molecule with a specific selectivity in mind, prior to the synthetic

*To whom correspondence should be addressed: (Phone) +82-2-880-8130, (FAX) +82-2-877-3025, (e-mail) dschung@snu.ac.kr
†Present Address: Materials and Process Simulation Center, California Institute of Technology, Mail Code BI 139-74, Pasadena, CA 91125, USA
‡Present address: Natural Science Research Institute, Jeonju University, Jeonju 560-759, Korea

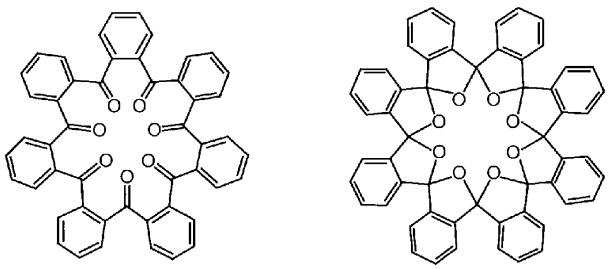

1 **2**

Figure 1. Structures of [1$_7$]ketonand (**1**) and of [1$_8$]starand (**2**).

effort of constructing the host.[19] A thorough understanding of ion–host interactions is also fundamental in comprehending the ion-binding mechanism in various biological processes.[3] With these purposes in mind, we performed free energy perturbation (FEP) and molecular dynamics (MD) simulations on the complexes of **1** with Li^+, Na^+, K^+, Rb^+, and Cs^+ in methanol, since both the alkali metal cations and the host **1** can be dissolved simultaneously in methanol and thus the results from the present report could be checked by experiments performed in methanol solvent.

Calculation Details

FEP simulation[20-22] has proven to be a useful tool in studying various host–guest systems.[2,19,23-26] It allows for the calculation of the free energy difference ($\Delta\Delta G$ or $\Delta\Delta A$) between two similar structures, such as the difference in binding free energies between two different ions bound to the same host molecules. Since the most important quantities in chemistry and biochemistry, such as binding constants (K) of host-guest complexes, are directly related to the Gibbs free energy ($\Delta G = -RT \ln K$ and $\Delta\Delta G = \Delta G_1 - \Delta G_2 = -RT \ln K_1/K_2$), the free energy calculation by employing FEP simulation is particularly useful in a direct comparison with experiment.[2,3,22,27,28] The thermodynamic cycle shown in Scheme 1 was used to calculate the relative binding Helmholtz free energy ($\Delta\Delta A$) between two cations M_1 and M_2 to a host H in the solvent phase. Since A is a state function, $\Delta\Delta A = \Delta A_1 - \Delta A_2 = \Delta A_3 - \Delta A_4$. The relative binding free energy ($\Delta\Delta A$) between a pair of cations M_1 and M_2 can be obtained by calculating the free energy changes (ΔA_3 and ΔA_4) for a perturbation or mutation of M_1 into M_2 in both free and bound forms, rather than by attempting the more difficult task of calculating those involved in the binding processes (ΔA_1 and ΔA_2).[20-23] A mutation from M_1 to M_2 was done by using a coupling parameter λ to smoothly convert the potential V of M_1 ($\lambda = 0$) into that of M_2 ($\lambda = 1$). A hypothetical intermediate potential V_λ is defined as $V_\lambda = (1 - \lambda) V_1 + \lambda V_2$ ($0 \leq \lambda \leq 1$). Dividing the range of λ into a number of discrete intermediate values (windows or Gaussian quadrature points), λ_i, the free energy change was calculated using the finite difference thermodynamic integration (FDTI) algorithm of Mezei[29,30] as follows:

$$\Delta A = A(\lambda = 1) - A(\lambda = 0)$$

$$= -RT \ln \left\langle \exp\left(-\frac{\Delta E}{RT}\right) \right\rangle_\lambda$$

$$= -RT \sum_{\lambda=0}^{1} \ln \left\langle \exp\left(-\frac{E(\lambda+\delta\lambda) - E(\lambda)}{RT}\right) \right\rangle_\lambda \qquad (1)$$

where the bracket denotes an average over an ensemble sampled during molecular dynamics (MD) or Monte Carlo (MC) simulations with a potential V_λ at $\lambda = \lambda_i$. In our simulations, we used the molecular dynamics (MD) simulations at constant volume to generate a canonical ensemble, and thus the Helmholtz free energy difference $\Delta\Delta A$ was obtained. The experimentally measured free energy difference is $\Delta\Delta G$, rather than $\Delta\Delta A$, and this should be obtained from the constant pressure simulation. However, considering that the $P\Delta(\Delta V)$ contribution in $\Delta\Delta G$ is small in the condensed phase for systems such as those we are interested in, direct comparison between our calculated results $\Delta\Delta A$ and the experimental data $\Delta\Delta G$ is warranted.[31] Harris and Loew had calculated both $\Delta\Delta A$ and $\Delta\Delta G$ in their FEP calculations, which gave very similar results to each other.[32]

All simulations were performed using the CVFF (Consistent Valence Force Field) force field implemented in the *Discover* molecular dynamics simulation package.[30] Parameters for alkali metal cations were converted from the AMBER parameters of Kollman[19] according to the formula, $A = \varepsilon(2R^*)^{12}$ and $B = 2\varepsilon(2R^*)^6$, and are listed in Table 1.[33,34] These parameters were taken from the work of Åqvist on alkali metal ions in water,[27] and Åqvist has shown that the solvation free energies of alkali metal ions in methanol calculated with these parameters were in good agreement with the experimental estimates.[27] These parameters have also been used in the FEP–MD work of Sun and Kollman on the K^+-complex of 18-crown-6 in methanol.[35]

All the FEP and MD simulations were carried out at 300 K with a time step of 1 fs. A periodic boundary condition was employed with a minimum image model, and a cutoff of 11 Å was used for nonbonding interactions. Throughout the simulations, the solvent molecules were treated explicitly using a 36.00 Å × 35.00 Å × 29.89 Å rectangular box whose size was adjusted to give a density of 0.79 g/cm^3 of methanol. It contained 560 methanol molecules. An all-atom representation was used for the methanol molecule. The arrangement of the solvent molecules was randomized and

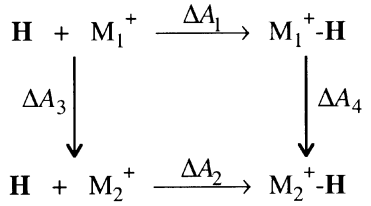

Scheme 1. Thermodynamic cycle for the ions M_1 and M_2 to a host **H**. ΔA_1 and ΔA_2 are the free energy changes involved in the binding processes of M_1^+ and M_2^+ to a host **H**. ΔA_3 and ΔA_4 are those involved in the mutation of M_1^+ into M_2^+ in unbound and host-bound forms, respectively.

Table 1. CVFF Parameters for Nonbonding Interactions of Alkali Metal Cations Converted from the AMBER Parameters of Kollman[19] According to the Formula. $A = \varepsilon(2R^*)^{12}$ and $B = 2\varepsilon(2R^*)^6$

	AMBER		CVFF	
	ε (kcal/mol)	R^* (Å)	A	B
Li	1.83×10^{-2}	1.137	349.8941	5.06085
Na	2.77×10^{-1}	1.868	20481.5198	15.06437
K	3.28×10^{-1}	2.658	167068.0913	14.80518
Rb	1.71×10^{-1}	2.956	309928.8651	14.51729
Cs	8.06×10^{-2}	3.395	774055.9141	15.79733

equilibrated by a 30-ps MD simulation, giving a stable potential energy. A bare alkali metal cation was then soaked into this solvent box with an overlapping solvent molecule removed. To represent an ion–host complex in methanol, the cation was located at the center of mass of **1**, and the complex was minimized and then soaked into the methanol solvent box with about 30 overlapping solvent molecules removed. It was minimized for 100 steps to remove any hot spots (any partial overlap between solvent and solute), and then pre-equilibrated for a period of 50 ps using MD simulation with a constraint that causes the solute to be located at the center of the solvent box.

Then, the FEP simulation was carried out to perturb Li^+ into Na^+, Na^+ into K^+, K^+ into Rb^+, and Rb^+ into Cs^+, respectively. 20 Gaussian quadrature points were used to go from the initial ($\lambda = 0$) to the final ($\lambda = 1$) state in each FEP simulation. At each point ($\lambda = \lambda_i$), MD simulation was carried out with a time step of 1 fs for 0.5 ps of equilibration and 1 ps of data collection. The calculated results were compared to those obtained with a time step of 1 fs for 1 ps of equilibration and 2 ps of data collection. All FEP simulations were run in both the forward (from $\lambda = 0$ to $\lambda = 1$) and the backward (from $\lambda = 1$ to $\lambda = 0$) directions in order to determine the hysteresis error as an estimate for the adequacy of the phase space sampling in our calculations.[21,22,36] Throughout this work, we assumed that the cation–counteranion salts were completely dissociated in the methanol solvent and that the cation and the host form a 1 : 1 complex.

Results and Discussion

Relative binding affinities for alkali metal cations: Free energy perturbation calculation. The FEP results are presented in Table 2, and Figure 2. The values obtained by 0.5 ps of equilibration and 1 ps of data collection at each point ($\lambda = \lambda_i$) showed almost the same trends as those obtained by 1 ps of equilibration and 2 ps of data collection, and thus we listed only the latter results in Table 2. The relative free energies of solvation of bare alkali metal cations in methanol (ΔA_3) are given in Table 2(a), and the relative free energies of solvation of alkali metal complexes of **1** in methanol are given in Table 2(b). These values are the average of forward and backward free energy simulations. The hysteresis errors are at most 0.2 kcal/mol in all simulations except for ($Li^+ \rightarrow Na^+$)-**1**, and these small errors along with the convergence of the relative binding affinities upon the doubling of simulation time, indicate that the length of the simulation was adequate to obtain proper sampling and to give a meaningful result.[21,22,36,37] The final results, the relative binding affinities of **1** for M_1^+ with respect to M_2^+ in methanol ($\Delta\Delta A$), are estimated by subtracting the relative solvation free energies of bare alkali metal cations (ΔA_3) from those of the alkali-complexes of **1** (ΔA_4). If $\Delta\Delta A = \Delta A_4 - \Delta A_3 - \Delta A_2 - \Delta A_1 > 0$ for ($M_1^+ \rightarrow M_2^+$) perturbation, the binding affinity of **1** in methanol is larger for M_1^+ than for M_2^+.

All the ΔA_3 values were calculated to be positive, and thus the stability of the metal cation in methanol is in the order $Li^+ > Na^+ > K^+ > Rb^+ > Cs^+$, which is in agreement with

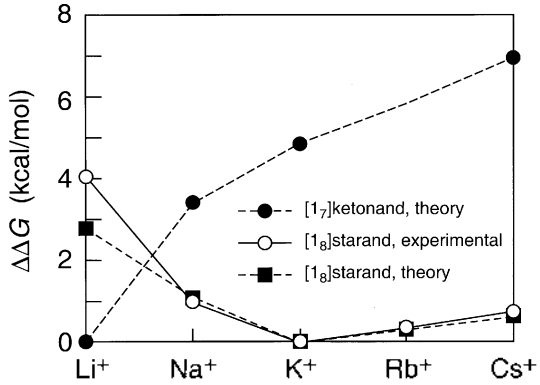

Figure 2. Results of the FEP calculation on the relative affinities of **1** and **2** toward alkali metal cations in methanol, which is a graphical representation of the data listed in Table 2. ● : calculated free energy change ($\Delta\Delta G$; in kcal/mol) during the complexation of **1** with each cation which are shown relative to that of **1** with Li^+; ■ : calculated free energy change during the complexation of **2** with the cations which are shown relative to that of **2** with K^+. : experimental free energy change during the complexation of **2** with the cations.

Table 2. Results of FEP Calculations for Alkali Metal Cation Complexes of **1** and **2** in Methanol (in kcal/mol)[a]

	(a) ΔA_3[b]	(b) ΔA_4[c]		(c) $\Delta\Delta A$[d]	
		1	**2**	**1**	**2**
$Li^+ \rightarrow Na^+$	$19.5_5 \pm 0.1_8$	$22._{96} \pm 1._{27}$	$17.8_6 \pm 0.4_1$	$3._{41} \pm 1._{28}$	$-1.6_9 \pm 0.4_5$
$Na^+ \rightarrow K^+$	$11.5_1 \pm 0.1_0$	$12.9_7 \pm 0.1_0$	$10.4_1 \pm 0.1_6$	$1.4_6 \pm 0.1_4$	$-1.1_0 \pm 0.1_9$
$K^+ \rightarrow Rb^+$	3.87 ± 0.04	$4.8_5 \pm 0.1_3$	4.19 ± 0.04	$0.9_8 \pm 0.1_4$	0.32 ± 0.06
$Rb^+ \rightarrow Cs^+$	5.04 ± 0.05	$6.1_7 \pm 0.1_6$	5.34 ± 0.06	$1.1_3 \pm 0.1_7$	0.30 ± 0.08

[a] A simulation time of 1 ps of equilibration and 2 ps of data sampling was used at each Gaussian quadrature point. The positive value in A → B means that A has a lower energy than B. [b] Relative solvation free energies of free cations in methanol. [c] Relative solvation of free energies of cations complexed with **1** and **2** in methanol. [d] Relative cation binding affinities of **1** and **2** in methanol ($\Delta\Delta A = \Delta A_4 - \Delta A_3$).

experimental[2,38,39] and other calculational results.[37] All the ΔA_4 values were positive and the stability of the cation complex of **1** is also in the order $Li^+ > Na^+ > K^+ > Rb^+ > Cs^+$. This indicates that Li^+ forms more stable complex with **1** in methanol than any other alkali cation, followed by Na^+ and K^+. However, the extent of the stabilization of Li^+ with respect to Na^+ (and of Na^+ with respect to K^+) is much larger in the complex with **1** than in the complex with **2**. Li^+-**1** is more stable than Na^+-**1** by 23 kcal/mol and Na^+-**1** is more stable than K^+-**1** by 13 kcal/mol. Li^+-**2** is more stable than Na^+-**2** only by 18 kcal/mol and Na^+-**2** is more stable than K^+-**2** only by 10 kcal/mol. As a result, the preference of **1** for Li^+ over Na^+ and for Na^+ over K^+ (ΔA_4: 23 and 13 kcal/mol, respectively) is large enough to compensate the preference of the methanol for Li^+ over Na^+ and for Na^+ over K^+ (ΔA_3: 19.6 and 11.5 kcal/mol, respectively), but the preferences of **2** for Li^+ over Na^+ and for Na^+ over K^+ (ΔA_4: 18 and 10 kcal/mol, respectively) are not high enough. The relative binding affinities ($\Delta\Delta A = \Delta A_4 - \Delta A_3$) of ($Li^+ \rightarrow Na^+$)-**1** and ($Na^+ \rightarrow K^+$)-**1** are positive and those of ($Li^+ \rightarrow Na^+$)-**2** and ($Na^+ \rightarrow K^+$)-**2** are negative. So the binding affinity is in the order $Li^+ > Na^+ > K^+ > Rb^+ > Cs^+$ for **1** and $K^+ > Rb^+ > Cs^+ > Na^+ > Li^+$ for **2**. The simulation result for **2** was in excellent agreement with the NMR experiments.[17]

Structure and energy of each complex: Molecular dynamics results. To explain the calculated selectivity of **1** for Li^+, Na^+, and K^+, we investigated the structures and energetics of the alkali metal complexes of **1** obtained from the trajectories of molecular dynamics simulations on these complexes. The average structures of the complexes are given in Figure 3, and the radial distribution function (RDF) $g(r)$ of the oxygen atoms around the alkali cation in each complex in methanol are given in Figures 4 and 5 in order to grasp the coordination details around the alkali cation. Comparing RDF with that of the bare cation in methanol, we can check out the change in coordination around the cation upon complexation. The coordination number (CN), $n(r)$, between the cation and the oxygen atoms as a function of the M^+-O distance was obtained by integrating the RDF.[24,32] This is also given in Figures 4 and 5. In order to see the details of energetics involved in these complexes, the interaction energy was decomposed into three components as follows:[3,33]

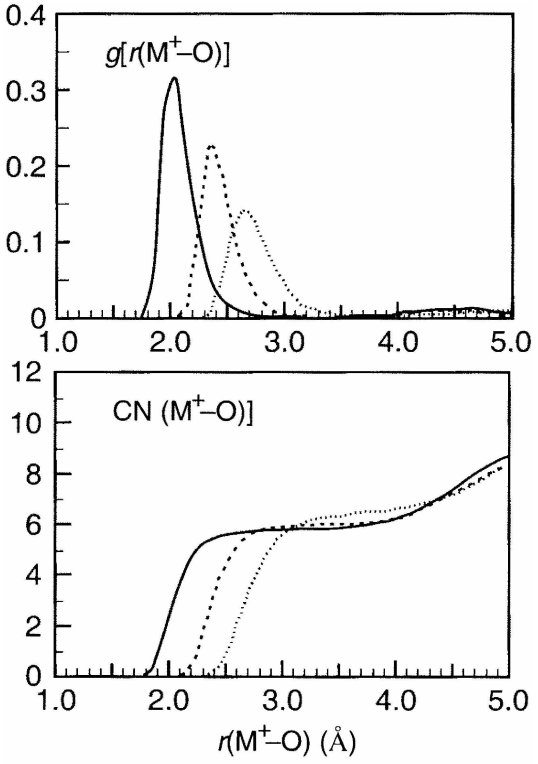

Figure 4. The radial distribution functions (upper) and the coordination number (lower) of the oxygen atoms around the cation M^+ in M^+-1 complex in methanol. Solid, dashed, and dotted lines represent Li^+-, Na^+-, and K^+-complexes, respectively.

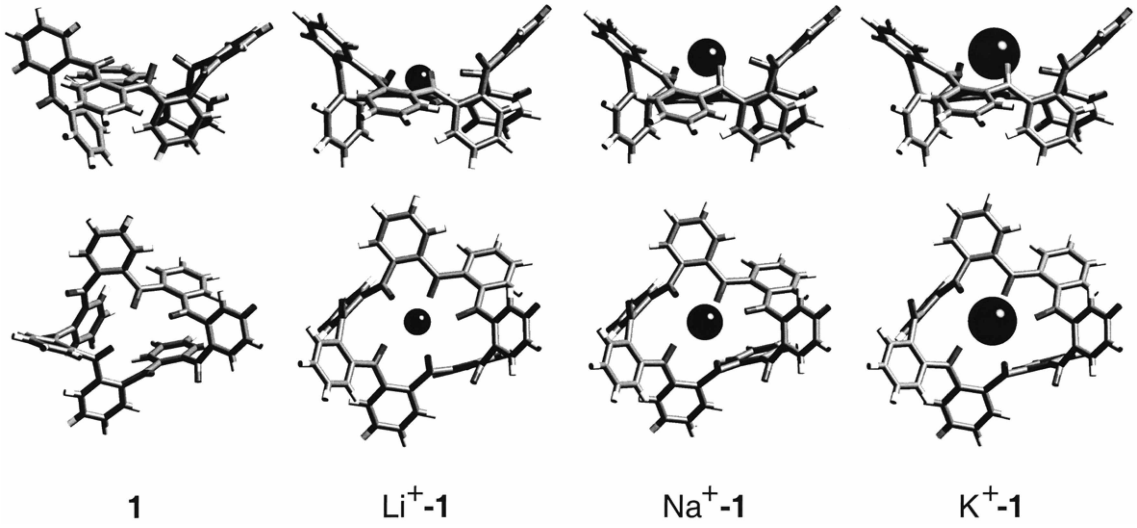

Figure 3. The average structures of the alkali complexes of 1 in methanol obtained from molecular dynamics simulations, along with those of **1** in methanol prior to complexation which were also obtained from the molecular dynamics simulations. Side view (upper) and top view (lower).

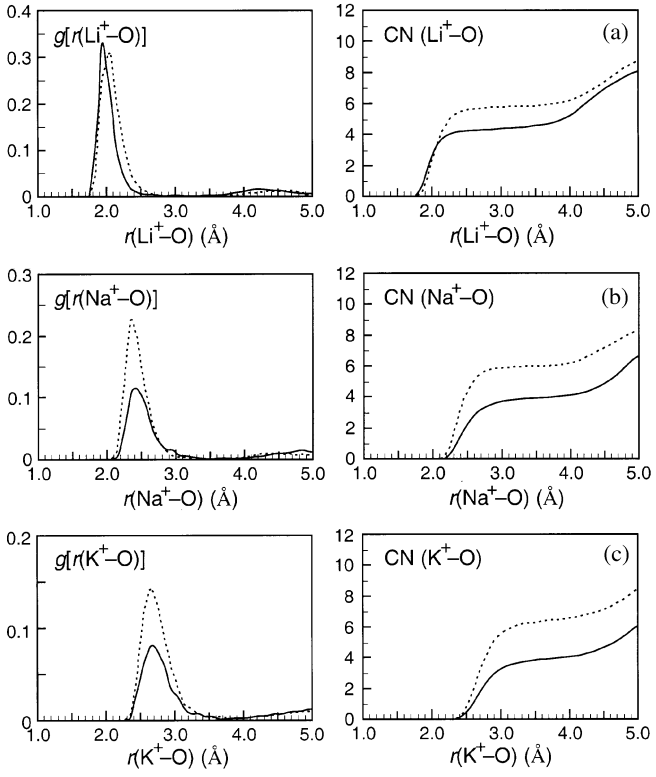

Figure 5. The radial distribution functions (left) and the coordination number (right) of the oxygen atoms around the cation M^+; (a) $M^+ = Li^+$, (b) Na^+, and (c) K^+. Solid and dashed lines represent the free M^+ in methanol, and M^+-**1** complex in methanol, respectively.

$$V_{total} = V_{Coulomb} + V_{vdW} + V_{intra} \quad (2)$$

where $V_{Coulomb}$ denotes the Coulombic energy component, V_{vdW} the van der Waals (vdW) energy component, and V_{intra} the sum of the bond-stretching, the angle, the dihedral angle, and the out-of-plane energy components. Since V_{intra} involves only the intramolecular energy components of a host, the amount of strain imposed on a host during the complexation can be judged from the change of this energy component. The decomposed energy components are listed in Table 3. The change in the total energy during complexation includes the cost of rearranging the host to accommodate the cation and the non-bonded Coulombic and vdW interactions between the cation and the host.

It is known that two principles generally govern the complexation process: complementarity and preorganization.[24] Complementarity involves the steric and electrostatic fit of host and guest, reflected in general by a cavity-shape cation-size relationship. In this work, the electrostatic and steric fit is characterized by the two terms: (1) the position of the first peak of M^+–O RDF and (2) the change in nonbonding energy components (Coulombic and vdW energy components) accompanied by complexation. By comparing the peak position of the M^+–O RDF with the optimal distance between the cation and oxygen, we can judge the complementarity. The optimal distance can be obtained from the peak position of RDF of bare cations in solvent,[24-28] or from the sum of the Pauling[40]/Shannon[41] ionic radii of the cation and oxygen.[3,42] Preorganization[43,44] is defined as the absence of structural reorganization upon complexation; the more the hosts are highly organized for binding, the more stable will be their complexes. The conformational modification arising from complexation results in decreased stability. In this work, the degree of preorganization is measured by (1) the root-mean-square (RMS) deviation of the host conformation before and after complexation, and (2) the change in the intramolecular (or strain) energy component of the host accompanied by the complexation.

Table 3. The Average Total Energies and their Components (in kcal/mol) of the Alkali Metal Complexes of **1** Obtained from Molecular Dynamics Simulations[a]

	Li^+-**1**→Na^+-**1**	Na^+-**1**→K^+-**1**
Total	30.36	9.62
Coulombic	37.68	19.46
vdW	2.80	2.28
Intramolecular[b]	−10.85	−12.53

[a]Only their differences between two different metal systems are listed. A positive value in A → B denotes that A has a lower energy than B. [b]Sum of the bond stretching, the angle, the dihedral angle, and the out-of-plane energy components. The higher value of this energy component indicates that the higher strain is imposed on the host.

The average structures of Li^+-, Na^+-, and K^+-complexes of **1** in methanol are given in Figure 3, along with those of **1** in methanol prior to complexation. The RMS deviation between the average structures of **1** before and after complexation was calculated as a measure of the extent of the conformational change of **1** induced during the complexation for the best fit of the alkali cation. It is found to be the largest for Li^+-**1**, and we can see that the smallest Li^+ induces the highest extent of conformational change of **1** for optimal coordination. The RDF of the oxygen atoms around the alkali cation in each complex in methanol is given in Figures 4 and 5. The maximum of the first peak of the M^+–O RDF is located at 2.05, 2.35, and 2.65 Å for Li^+-**1**, Na^+-**1**, and K^+-**1**, respectively. These positions correspond to those of the first peak of M^+–O RDF of bare M^+ in methanol, as shown in Figure 5. These values are also close to the sum of Pauling crystal radii (2.00, 2.35, and 2.73 Å)[3,40,45] and the sum of Shannon crystal radii (2.16, 2.42, and 2.78 Å)[41] of alkali metal M^+ and oxygen atom when M^+ is Li^+, Na^+, and K^+, respectively. These results indicate that the carbonyl oxygen atoms constituting the central cavity of **1** can be rearranged to make optimal interactions with all the alkali metals. The rearrangement of carbonyl groups of **1** brings about almost the same oxygen environment around the cation of M^+-**1** complex in methanol as the bare M^+ in methanol for each M^+.[24] The carbonyl oxygen atoms in **1** can wrap even around the smallest Li^+. As a result, the smallest Li^+ and the negatively charged oxygen atoms are located in very close proximity, and the electrostatic interaction between the cation and **1** is expected to be the most favorable for Li^+-**1**, followed by Na^+-**1** and then by K^+-**1**.

This is confirmed from the average Coulombic energy component given in Table 3. The Coulombic energies of Li^+-**1** and Na^+-**1** are lower than those of Na^+-**1** and K^+-**1** by 37.7 and 19.5 kcal/mol, respectively. The CN of oxygen atoms around the cation increases during the complexation with **1**, and the nature of this increase is different for each complex as shown in Figure 5. The CNs up to the first coordination shell were about six for Li^+-**1** and Na^+-**1** and slightly greater than six for K^+-**1**, of which five oxygen atoms are from **1** and one from the methanol solvent. The corresponding CNs were about four for bare Li^+, Na^+, and K^+ in methanol. Unlike Li^+-**1**, the CN in Na^+-**1** and K^+-**1** increases more rapidly than in bare Na^+ and K^+, and thus more oxygen atoms crowd at the first coordination shell around Na^+ and K^+ in Na^+-**1** and K^+-**1** than in bare Na^+ and K^+. This crowding effect can cause an unfavorable repulsive vdW interactions in Na^+-**1** and K^+-**1**. Therefore, it is expected that the vdW interaction is the most favorable for Li^+-**1**, followed by Na^+-**1** and then by K^+-**1**. This is confirmed by the average vdW energy components given in Table 3. The vdW energies of Li^+-**1** and Na^+-**1** are lower than those of Na^+-**1** and K^+-**1** by 2.8 and 2.3 kcal/mol, respectively. Since the conformational change of **1** induced during the complexation for the best fit of the alkali cation is the largest for Li^+-**1**, it is expected that the energy cost, *i.e.*, the strain for achieving the optimal conformation of the host is the largest for Li^+-**1**. The intramolecular energy component V_{intra}, as a measure of strain imposed on **1**, is listed in Table 3. The amounts of strain imposed on Li^+-**1** and Na^+-**1** are larger than those on Na^+-**1** and K^+-**1** by 10.9 and 12.5 kcal/mol, respectively. However, these energy costs are not large enough to change the selectivities of **1** toward alkali cations, which is determined by the dominant Coulombic components.

Concluding Remarks

We performed free energy perturbation and molecular dynamics simulations to obtain the relative binding affinities of [1$_7$]ketonand (**1**) toward alkali metal cations in methanol. FEP simulations gave the selectivity $Li^+ > Na^+ > K^+ > Rb^+ > Cs^+$ for **1**. The highest affinity of **1** for Li^+ was predominantly due to the Coulombic attractions between the smallest Li^+ and the carbonyl oxygens comprising the central cavity of **1** since the carbonyl groups of **1** wrap around even the smallest Li^+ without causing serious strain on **1**.

Acknowledgment. This work is supported by the Korea Science and Engineering Foundation (KOSEF: 96-0501-08-01-3) and the Basic Science Research Institute Program (BSRI-97-7402). S. H. acknowledges a postdoctoral research fellowship by the Korea Research Foundation.

References

1. Dugas, H. *Bioorganic Chemistry: A Chemical Approach to Enzyme Action*, 3rd ed.; Springer-Verlag, Inc.: New York, 1996.
2. Grootenhuis, P. D. J.; Kollman, P. A. *J. Am. Chem. Soc.* **1989**, *111*, 2152-2158.
3. Eisenman, G.; Alvarez, O.; Aqvist, J. *J. Inclusion Phenom. Mol. Recognit. Chem.* **1992**, *12*, 23-53.
4. Quici, S.; Manfredi, A.; Raimondi, L.; Sironi, A. *J. Org. Chem.* **1995**, *60*, 6379-6388.
5. Cox, B. G.; Schneider, H. *Coordination and Transport Properties of Macrocyclic Compounds in Solution*; Elsevier Science Publishers B. V.: Amsterdam, 1992; Vol. 76.
6. Carmichael, V. E.; Dutton, P. J.; Fyles, T. M.; James, T. D.; McKim, C.; Swan, J. A.; Zojaji, M. Biomimetic Ion Transport: Pores and Channel in Vesicle Membranes. In *Inclusion Phenomena and Molecular Recognition*; Atwood, J. L., Ed.; Plenum Press: New York and London, 1990; pp 145-150.
7. Thompson, M. A.; Glendening, E. D.; Feller, D. *J. Phys. Chem.* **1994**, *98*, 10465-10476.
8. Cram, D. J.; Chapoteau, E.; Czech, B. P.; Gebauer, C. R.; Helgeson, R. C.; Kumar, A. Novel Chromogenic Ionophores for Determination of Sodium and Potassium in Biological Fluids: Synthesis and Applications. In *Inclusion Phenomena and Molecular Recognition*; Atwood, J. L., Ed.; Plenum Press: New York and London, 1990; pp 217-225.
9. Lee, W. Y. *Synlett* **1994**, 765-776.
10. Lee, W. Y.; Park, C. H.; Kim, S. *J. Am. Chem. Soc.* **1993**, *115*, 1184-1185.
11. Lee, W. Y.; Park, C. H.; Kim, H.-J.; Kim, S. *J. Org. Chem.* **1994**, *59*, 878-884.
12. Lee, W. Y.; Park, C. H. *J. Org. Chem.* **1993**, *58*, 7149-7157.
13. Hwang, S.; Ryu, G. H.; Lee, K. H.; Hong, J.-I.; Chung, D. S. *Bull. Korean Chem. Soc.* **1998**, *19*, 406-408.
14. Hwang, S.; Ryu, G. H.; Jang, Y. H.; Chung, D. S. *Bull. Korean Chem. Soc.* In Press.
15. Cho, S. J.; Hwang, H. S.; Park, J. M.; Oh, K. S.; Kim, K. S. *J. Am. Chem. Soc.* **1996**, *118*, 485-486.
16. Cui, C.; Cho, S. J.; Kim, K. S. *J. Phys. Chem. A* **1998**, *102*, 1119-1123.
17. Hwang, S.; Lee, K. H.; Ryu, G. H.; Jang, Y. H.; Lee, S. B.; Lee, W. Y.; Hong, J.-I.; Chung, D. S. *Submitted for publication (J. Org. Chem.)*.
18. Ungaro, R.; Arduini, A.; Casnati, A.; Ori, O.; Pochini, A.; Ugozzoli, F. Complexation of Ions and Neutral Molecules by Functionalized Calixalenes. In *Computational Approaches in Supramolecular Chemistry*; Wipff, G., Ed.; Kluwer Academic Publishers: Dordrecht, 1994; pp 277-300.
19. Bayly, C. I.; Kollman, P. A. *J. Am. Chem. Soc.* **1994**, *116*, 697-703.
20. Kollman, P. *Chem. Rev.* **1993**, *93*, 2395-2417.
21. van Gunsteren, W. F.; Mark, A. E. *Eur. J. Biochem.* **1992**, *204*, 947-961.
22. van Gunsteren, W. F. *Protein Eng.* **1988**, *2*, 5-13.
23. Cummins, P. L.; Ramnarayan, K.; Singh, U. C.; Gready, J. E. *J. Am. Chem. Soc.* **1991**, *113*, 8247-8256.
24. Miyamoto, S.; Kollman, P. A. *J. Am. Chem. Soc.* **1992**, *114*, 3668-3674.
25. Burger, M. T.; Armstron, A.; Guarnieri, F.; McDonald, D. Q.; Still, W. C. *J. Am. Chem. Soc.* **1994**, *116*, 3593-3594.
26. McDonald, D. Q.; Still, W. C. *J. Am. Chem. Soc.* **1996**, *118*, 2073-2077.
27. Aqvist, J.; Alvarez, O.; Eisenman, G. *J. Phys. Chem.* **1992**, *96*, 10019.

28. Glendening, E. D.; Feller, D. *J. Am. Chem. Soc.* **1996**, *118*, 6052-6059.
29. Mezei, M. *J. Chem. Phys.* **1987**, *86*, 7084-7088.
30. *Discover User Guide, version 95.0*; Biosym Technologies: San Diego, 1995.
31. Fleischman, S. H.; Brooks, I. C. L. *J. Chem. Phys.* **1987**, *87*, 3029-3037.
32. Harris, D.; Loew, G. *J. Comput. Chem.* **1996**, *17*, 273-288.
33. Cummins, P. L.; Gready, J. E. *J. Comput. Chem.* **1994**, *15*, 704-718.
34. Molecular Simulations Scientific Support. http://www.msi.com/support/discover/forcefield/add_nonbond.html (accessed March 1997).
35. Sun, Y.; Kollman, P. A. *J. Am. Chem. Soc.* **1995**, *117*, 3599-3604.
36. Mitchell, M. J.; McCammon, J. A. *J. Comput. Chem.* **1991**, *12*, 271-275.
37. Thomas IV, B. E.; Kollman, P. A. *J. Am. Chem. Soc.* **1994**, *116*, 3449-3452.
38. Markus, Y. *Ion Solvation*; Wiley & Sons: New York, 1985.
39. Burgess, M. A. *Metal Ions in Solution*; Ellis Horwood, Ltd.: England, 1978.
40. Pauling, L. *The Nature of the Chemical Bond and the Structure of Molecules and Crystals: An Introduction to Modern Structural Chemistry*; 3rd ed.; Cornell University Press: Ithaca, New York, 1960.
41. Shannon, R. D. *Acta Crystallogr.* **1976**, *A32*, 751.
42. Fronczek, F. R.; Gandour, R. D. Crystallography of Cation Complexes of Lariat Ethers. In *Cation Binding by Macrocycles: Complexation of Cationic Species by Crown Ethers*; Inoue, Y., Gokel, G. W., Eds.; Marcel Dekker, Inc.: New York and Basel, 1990; pp 311-361.
43. Cram, D. J. *Science* **1988**, *240*, 760-767.
44. Dietrich, B.; Viout, P.; Lehn, J.-M. *Macrocyclic Chemistry: Aspects of Organic and Inorganic Supramolecular Chemistry*; VCH: Weinheim, 1993.
45. Åqvist, J. *J. Phys. Chem.* **1990**, *94*, 8021-8024.